Surfactant flooding: The influence of the physical properties on the recovery efficiency

Druetta, Pablo; Picchioni, Francesco

Published in:
Petroleum

DOI:
10.1016/j.petlm.2019.07.001

Publication date:
2019

Petroleum 6 (2020) 149–162

Contents lists available at ScienceDirect

Petroleum

journal homepage: http://www.keaipublishing.com/en/journals/petroleum

Surfactant flooding: The influence of the physical properties on the recovery efficiency

P. Druetta, F. Picchioni*

Department of Chemical Engineering, ENTEG, University of Groningen, Nijenborgh 4, 9747AG, Groningen, the Netherlands

ARTICLE INFO

Keywords:
EOR
Surfactant
Adsorption
Reservoir simulation
Total variation diminishing

ABSTRACT

Enhanced Oil Recovery (EOR) processes aim at increasing the performance and operative life of oilfields while newer, greener and more efficient energy sources are developed. Among the chemical EOR techniques, surfactant flooding is one of the most well-known methods, applied mainly in low- and medium-viscosity oilfields. Surfactants diminish the interfacial energy between the oleous and aqueous phases, reducing the forces responsible of the capillary trapping phenomenon and mobilizing the remaining oil. This paper presents the study of a novel two-dimensional surfactant flooding simulator for a four-component (water, petroleum, chemical, salt), two-phase (aqueous, oleous) system in porous media. It is aimed mainly at discussing the influence of the physical phenomena present in the reservoir during the recovery, namely: rock compressibility, diffusion, capillary pressure and adsorption. The system is numerically solved using a second-order finite difference method using the IMPEC (IMplicit Pressure and Explicit Concentration) scheme. The oil recovery factor was negatively affected when these phenomena were considered, being strongly sensitive to the adsorption. The other phenomena decreased the efficiency of the process to a lesser extent, whilst the capillary pressure did not affect significantly the flooding performance. The presence of salt in the reservoir rendered the adsorption process more relevant, with water-in-oil emulsions being more sensitive to the presence of this fourth component. This paper shows the importance of the design and optimization of chemical agents to be used in EOR before its field application.

1. Introduction

Crude oil and its derivatives have been for the last 150 years the main source of energy and raw material for the industrial processes, and nowadays the economies still depend largely on its continuous supply [1–4]. The exploitation of oil fields can be divided in three main stages, according to the mechanisms involved in the recovery: the primary stage uses natural driven mechanisms (e.g., expansion drive, compaction, gravitational), followed by the secondary, or waterflooding, in which a fluid is injected to repressurize and mobilize the oil to the producers [3,5–7]. After these two stages approximately 50% of the original oil in place (OOIP) still remains trapped underground due to several physical mechanisms (e.g., capillary forces). Tertiary recovery processes, also known as Enhanced Oil Recovery (EOR), aim at modifying one or several of the properties in the reservoir in order to mobilize part of this remaining oil [8]. There are several techniques, which depend mainly on the crude oil and rock formation, namely [6]: thermal (combustion in-situ - continuous/cyclic steam injection); chemical (polymers, surfactants and/or caustic); miscible (CO_2 injection, inert gas or miscible-solvent); and others (e.g., microbial EOR).

Among these, chemical EOR (CEOR) is mostly used for low and medium viscosity crude oils and, more importantly, they can also be employed in a wide range of rock formations. An important synergy between reservoir simulation and chemical EOR is that the numerical models can be used either to predict the performance or to set the requirements of the future chemical agents to be synthesized. In a previous paper, a novel surfactant simulator was presented in order to study a EOR sweeping process in an oil field. This study aims at extending this study, analyzing the influence of different physical phenomena (e.g., adsorption, diffusion, capillary pressure) on the recovery process. This simulator was designed to study a 2D oil field [9–11], to simulate a two-phase, four-component flow.

Peer review under responsibility of Southwest Petroleum University.
* Corresponding author.
E-mail addresses: p.d.druetta@rug.nl (P. Druetta), f.picchioni@rug.nl (F. Picchioni).
URL: http://www.rug.nl/research/product-technology/ (F. Picchioni).

https://doi.org/10.1016/j.petlm.2019.07.001
Received 16 August 2018; Received in revised form 15 March 2019; Accepted 2 July 2019

Nomenclature

Ad	Component Adsorption [day^{-1}]
c_r	Rock Compressibility [Pa^{-1}]
$\underline{\underline{D}}$	Dispersion Tensor
dm	Molecular Diffusion [m^2/s]
dl	Longitudinal Dispersion [m^2/s]
dt	Transversal Dispersion [m^2/s]
F_{LIM}	Flux Limiting Function
K	Absolute Permeability [mD]
k_r	Relative Permeability
p	Reservoir Pressure [Pa]
p_{wf}	Bottomhole Pressure [Pa]
q	Flowrate [m^3/day]
r_w	Well Radius [m]
S	Phase Saturation
s	Well Skin Factor
u	Darcy Velocity [m/day]
V	Volumetric Concentration
z	Overall Concentration

Greek Letters

Γ	Domain Boundary
δ_{ij}	Kronecker Delta
λ	Phase Mobility [m^2/(Pa· s)]
μ	Absolute Viscosity [Pa· s]
σ	Interfacial Tension [mN/m]
φ	Formation Porosity
Ω	Reservoir Domain

Superscripts

a	Aqueous Phase
c	Capillary
H	Water-Oil System (no Chemical)
j	Phase
$\langle n \rangle$	Time-Step
o	Oleous Phase
r	Residual

Subscripts

c	Surfactant Component
i	Component
in	Injection
m, n	Spatial Grid Blocks
p	Petroleum Component
s	Salt Component
t	Total
w	Water Component

1.1. Surfactant flooding

The use of surfactants for EOR is not a new technology, but has been used for more than 40 years [7,12–19]. Surfactants adsorb on the oil/water interface, reducing the interfacial tension (IFT) and capillary forces, which are responsible for the trapping phenomena in pores [20–22]. The interesting part about surfactants is its hydro- and lipophilicity, what makes them useful in immiscible, multiphase systems. The goal when designing surfactants for EOR is to achieve low interfacial tension at low surfactant concentrations, and low adsorption levels on the formation rock [23,24]. The numerical modeling of surfactant flooding, as in other chemical EOR processes, is generally done following the compositional approach [25–27]. These models have been employed during the last 50 years to model chemical EOR processes where other mathematical models (e.g., black-oil) cannot represent accurately the phase properties, behavior and mass transport of the different components present in the reservoir. Nolen [28] developed one of the first compositional simulators. This model was focused on describing a three dimensional reservoir and used a number of correlations to calculate its different physical properties such as densities, viscosities, and equilibrium *K*-values. Moreover, he also dealt with the problem of numerical dispersion. Using the method-of-characteristics, he demonstrated a way to minimize this issue in multicomponent miscible displacement problems. This simulator was validated presenting comparisons between with experimental data. Pope and Nelson [29,30] were among the first to report the importance of phase behavior in chemical flooding processes. They developed a one-dimensional compositional simulator to simulate the recovery of oil using different chemicals, such as surfactant and polymer. In the case of surfactant flooding, phase behavior and interfacial tension were modeled as functions of salinity and chemical concentration. The results reported included up to six components and up to three phases, using simplified representations of the binodal and distribution curves for the surfactant/brine/oil system. In spite of these simplifications, as many as 64 parameters are required to describe the flooding process. Porcelli [31–33] and Bidner [34] developed and tested a 1D chemical flooding simulator for a two-phase, three-component system. The capabilities included phase behavior, interfacial tension, residual saturations, relative permeabilities, phase viscosities, wettability, capillary pressure, adsorption and dispersion. The phase behavior was modeled based on simplifications of ternary diagrams, and the properties expressed as functions of the component partitioning constants, which depend on the type of surfactant used. They modeled Type II(−) and Type II(+) phase behaviors and tested the influence of the above-mentioned properties as well as the numerical discretization in the oil recovery factor. The results proved that in surfactant EOR processes, wettability alteration plays a key role in oil recovery from the reservoir. The phase behavior was relatively simple and considered that there was no surfactant partitioning, with the chemical species only present in the water phase, whilst the oleous phase is only composed by the oil species.

1.2. Aim of this work

The novelty of this work resides in extending the study presented in a previous paper, complementing the studies therein in order to study the influence of other physical phenomena in the EOR process using surfactants. These models represent an improvement of a previous 2D, three-component simulator for surfactant flooding [9]. The component partitioning is modeled in an accurate, but yet relatively simple and robust way, solving the stability problems present in previous simulators. Since in this study the salt is also considered in the system, the surfactant partitioning is expressed as a piece-wise function of the total dissolved solids (TDS) in the aqueous phase. The component partitioning then is modeled in the simulator the minimum number of parameters possible to describe the chemical behavior, avoiding the creation of a complex system of non-linear equations which would complicate the numerical solving, but at the same time preventing the oversimplification of the system, which would affect the recovery results.

The combination of the above-mentioned has resulted in a novel and complete simulator, which can be used for the design and screening of new surface active agents to be used in EOR. In order to understand how to increase the efficiency of the surfactant a series of numerical simulations were performed, aimed at analyzing how different

phenomena (excluding the phase behavior) affect the surfactant efficiency. Finally, the last part of the paper consists in presenting the results of a series of EOR flooding with surfactant when the salt is present as the fourth component in the system, modifying the phase behavior and the adsorption rates. Nonetheless, the current 2D model does not allow to consider the volumetric sweeping efficiency of EOR agents and how the difference in the densities between oil and EOR agents affects the efficiency of the process, specifically when the vertical permeability component cannot be neglected with respect to horizontal ones. Moreover, the influence of the temperature and heat transfer is not considered in the model, which affects the phases' rheological behavior and hence the mobility ratio as well as the influence of the salinity in the surfactant flooding. Furthermore, the compositional model is limited to two phases, neglecting the presence of the gas phase, which is usually present in many reservoirs. The mentioned phenomena should be the objective of further improvements, solving the current disadvantages with respect to commercial reservoir simulators.

The simulation of multiphase, multicomponent flow in porous media usually requires solving a number of coupled, non-linear system of equations dealing with temporal and spatial partial derivatives of pressure and mass concentrations. In the model it is adopted a fully second-order accuracy discretization scheme, along with a Total Variation Diminishing (TVD) flux limiter, which notoriously reduces the influence of numerical diffusion and dispersion mechanisms [11]. Generally speaking, commercial simulators present usually more advantages than academic ones. However, the objective of this paper is to present a novel chemical EOR reservoir simulator. The second-order accuracy in the discretization of the differential equations allows obtaining better results than standard academic simulators and moreover, it is comparable to commercial ones. Chemically speaking, the usage of the ternary diagram in order to model the phase behavior and the influence of the salinity on the calculation of the partition coefficient and on the phases' rheological behavior (e.g. calculation of aqueous viscosity in a step-wise approach considering the influence of all the components) were never considered in the academic simulators, and some of these are not considered by commercial ones. All in all, mathematically speaking the model represents a novelty with respect to academic simulators and chemically speaking, it represents an advance compared to academic simulators and presents some minor advantages against commercial simulators. Nevertheless, a major disadvantage with respect to the latter is the number of dimensions employed, although it is considered that a 2D approach is appropriate for a first development of the simulator in order to study the behavior of chemical agents. Moreover, this approach will allow studying the chemical performance in different oilfields in order to determine the set of desired properties when synthesizing new EOR agents.

1.3. Physical model

The physical model represents an oil field (Ω) of known geometric characteristics, with an absolute permeability tensor (K) and porosity (φ) (Fig. 1). These can be constant or represented by a normally distributed fields, with the porosity being also affected by the rock compressibility. The flow is considered isothermal, Newtonian, incompressible and 2-dimensional (it is assumed as in previous models that the vertical permeability is negligible when compared to horizontal ones). It is also assumed that the system is in local thermodynamic (phase) equilibrium. Finally, gravitational forces are negligible compared to the viscous and capillary forces [34].

Surfactant EOR flooding, such as other chemical techniques, involves the flow of fluids in two phases (aqueous and oleous), and various components (water, salt, chemical and petroleum). It is noteworthy that these components can be mixtures of a number of pure components, since petroleum is a mixture of many hydrocarbons, water contains dissolved monovalent and divalent salts and the surfactant is composed by a number of different molecules (e.g., cosurfactants) [3,8,16]. The recovery process involves injecting firstly a surfactant slug along with the aqueous phase, and subsequently a water bank is injected (pure water or brine) in order to drive the chemical slug, sweeping the mobilized oil into the producing wells. This model is represented by a system of strongly nonlinear partial differential equations which are completed by a set of algebraic relationships representing physical properties of the fluid and the rock, which are: component partitioning as a function of the salinity, interfacial tension, residual phase saturations, relative permeabilities, rock wettability, phase viscosities, capillary pressure, adsorption on the formation, and dispersion. As mentioned, the compressibility of the formation is also taken into account in the simulator. Underground porous media are subject to internal and external stresses due to the forces acting on the system. Internal ones are caused mainly from the fluids' pressure field, whilst external stresses are originated from gravitational forces and tectonic events, if any [10,35]. The numerical technique adopted for the resolution of these equations is the IMPEC method, which calculates pressures implicitly and concentration for each of the component explicitly. Improving the discretization methods presented in the literature [36], a fully second-order accuracy scheme is adopted in the model. Moreover, a flux limiter function is implemented in order to track more accurately the components throughout the reservoir [31,33,37,38].

1.4. Mathematical model

The flow of porous media can be studies from two different perspectives: the direct and the continuum approaches. The first one involves solving the Navier-Stokes equations and a detailed characterization of the poral geometry, which limits considerable its application. The continuum divided the domain in elementary volumes, averaging the properties, without the need of modeling the system at a poral-scale. In this case the Darcy law applies along with the mass transport equation. The compositional reservoir simulation uses this last approach, which offers the versatility to model a number of components present in the phases. This simulator is part of a series of models aimed at studying chemical EOR processes. Thus, this is an extension of a previously published simulator for surfactant flooding, which was validated against commercial and academic simulators under different configurations, discussing also its order of convergence (Fig. 2) [9,11]. Therefore, it is considered that the validation of this model was already done and reported [39–41]. The equations defining the flow in porous media are then (along with the dispersion tensor) [39–43],

$$\vec{u}^{\,j} = -\underline{K}\cdot\frac{k_r^j}{\mu^j}\cdot\vec{\nabla}p^j;\ j = o,\ a \tag{1}$$

$$\frac{\partial(\varphi z_i)}{\partial t} + \nabla\cdot\sum_j V_i^j\cdot\vec{u}^{\,j} - \nabla\cdot\sum_j \underline{\underline{D_i^j}}\cdot\nabla\cdot V_i^j = -\frac{\partial(\varphi A d_i)}{\partial t} + q_i;\ i = p,\ c,\ w,\ s \tag{2}$$

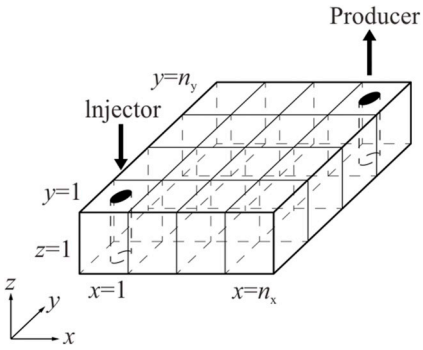

Fig. 1. Schematic representation of the quarter 5-spot used for the EOR surfactant flooding [9].

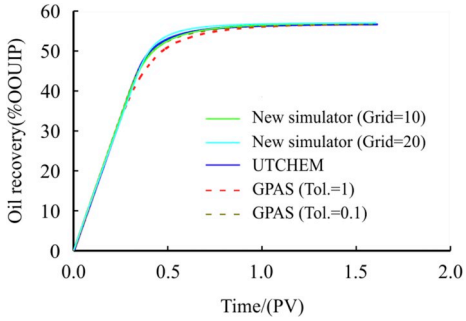

Fig. 2. Oil recovery during a 2D flooding, comparing the results of this simulator against UTCHEM and GPAS [11].

$$\underline{\underline{D_i^j}} = dm_i^j \cdot \varphi \cdot S^j \cdot \delta_{ij} + \|\vec{u}^j\| \cdot \left[\frac{dl^j}{\|\vec{u}^j\|^2} \cdot \begin{vmatrix} (u_x^j)^2 & u_x^j \cdot u_y^j \\ u_y^j \cdot u_x^j & (u_y^j)^2 \end{vmatrix} + dt^j \cdot \begin{vmatrix} 1 - \frac{(u_x^j)^2}{\|\vec{u}^j\|^2} & -\frac{u_x^j \cdot u_y^j}{\|\vec{u}^j\|^2} \\ -\frac{u_y^j \cdot u_x^j}{\|\vec{u}^j\|^2} & 1 - \frac{(u_y^j)^2}{\|\vec{u}^j\|^2} \end{vmatrix} \right] \tag{3}$$

$$\varphi c_r \frac{\partial p^a}{\partial t} + \vec{\nabla} \cdot (\lambda \cdot \nabla p^a) = \frac{\partial}{\partial t} \left(\varphi \cdot \sum_i Ad_i \right) - \vec{\nabla} \cdot (\lambda^o \cdot \nabla p_c) + q_t \tag{4}$$

2. Physical properties

2.1. Chemical component partition

As it is mentioned in the literature, the most relevant part of the analysis in surfactant flooding is to understand how the components distribute into the phase, what it is called phase behavior of the system. In this model, this is represented in a ternary phase diagram. The composition of a mixture is determined by any point inside the triangle, which is known with two of the total concentrations of the components [32,38,44–46]. As the concentration of the chemical increases, oil and water become miscible, so that the triangle can be divided into two zones (in two-phase systems): upper miscible and immiscible in the bottom. The curves delimiting these regions are determined by volumetric concentration ratios calculated as,

$$\text{Solubilization Coefficient} = L_{pc}^a = \frac{V_p^a}{V_c^a} \tag{5}$$

$$\text{Swelling Coefficient} = L_{wc}^o = \frac{V_w^o}{V_c^o} \tag{6}$$

$$\text{Partition Coefficient} = k_c = \frac{V_c^o}{V_c^a} \tag{7}$$

Depending on the value of k_c, two different behaviors are observed in two-phase systems: Type II(−) (for $k_c < 1$), and Type II(+) (for $k_c > 1$). The partition coefficient value, as reported previously, depends on the composition of the injected chemical and the water characteristics, such as temperature and salinity, and it is the most critical parameter affecting the surfactant performance. Sheng [47] described this two-phase approximation to surfactant flooding and the dependence on the salinity of the partition coefficient using a piece-wise function (Eq. (8) and Fig. 3) to describe this [35],

$$k_c = \begin{cases} 10^{2(V_s^a/V_{s,opt}^a - 1)} & \textbf{if} \quad V_s^a > V_{s,opt}^a \\ 10^{2(1 - V_s^a/V_{s,opt}^a)} & \textbf{if} \quad V_s^a < V_{s,opt}^a \end{cases} \tag{8}$$

In this case it is assumed that all the salinity present in the reservoir is composed by monovalent cations. The salt component is only present

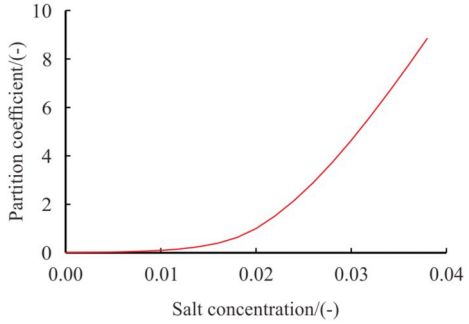

Fig. 3. Partition coefficient dependence on the salinity. In this example, according to Eq. (8), the optimum volumetric concentration of salt in water ($V_{s,opt}^a$) is equal to 2%.

in the aqueous phase ($V_s^o = 0$). With these relationships the system becomes numerically determined with a unique solution, and the parameters previously introduced can now be calculated for each representative elementary volume (REV). Fig. 4 shows the original and simplified ternary diagrams used for this simulation.

2.2. Interfacial tension

The interfacial tension of the system depends on the presence and concentration of the chemical component as well as the emulsion type present in the reservoir. In this simulation a simplified IFT correlation will be used [31–34,37].

For Type II(−) systems (oil/water emulsion):

$$\begin{aligned} &\log(\sigma) = \log(F) + (1 - L_{pc}^a) \cdot \log(\sigma^H) + \frac{G_1}{1 + G_2} \cdot L_{pc}^a;\ L_{pc}^a < 1 \\ &\log(\sigma) = \log(F) + \frac{G_1}{1 + L_{pc}^a \cdot G_2};\ L_{pc}^a \geq 1 \end{aligned} \tag{9}$$

For Type II(+) systems (oil emulsion/water):

$$\begin{aligned} &\log(\sigma) = \log(F) + (1 - L_{wc}^o) \cdot \log(\sigma^H) + \frac{G_1}{1 + G_2} \cdot L_{wc}^o;\ L_{wc}^o < 1 \\ &\log(\sigma) = \log(F) + \frac{G_1}{1 + L_{wc}^o \cdot G_2};\ L_{wc}^o \geq 1 \end{aligned} \tag{10}$$

where G_1 and G_2 are input parameters, and the term F is the correction factor introduced by Hirasaki, calculated according to the following equation:

$$F = \frac{1 - e^{-\sqrt{\sum_{i=p,w,c} (V_i^o - V_i^a)^2}}}{1 - e^{-\sqrt{2}}} \tag{11}$$

In chemical recovery process, the presence of the surfactant causes the decrease of IFT, allowing the mobilization of oil trapped in the reservoir, so it can be inferred that the residual saturations of the phases depend on the IFT. The IFT of the water-oil system (no surfactant present) is considered constant throughout the simulation.

2.3. Residual saturation

Residual saturations play an important role in oil recovery processes. They establish a certain limit to how much oil can be mobilized during the process. If such saturations can be reduced, this will increase the efficiency of the whole process. As explained in the previous section, they depend on the IFT in the water-oil two-phase system. The presence of the surfactant can modify the residuals saturations in the porous medium. This relationship is ruled by a dimensionless group, the capillary number, defined by the following equation:

$$N_{vc} = \frac{u \cdot K}{\lambda \cdot \sigma} \tag{12}$$

The functionality between the capillary number and the residual saturation for both phases is described by the following model [34]:

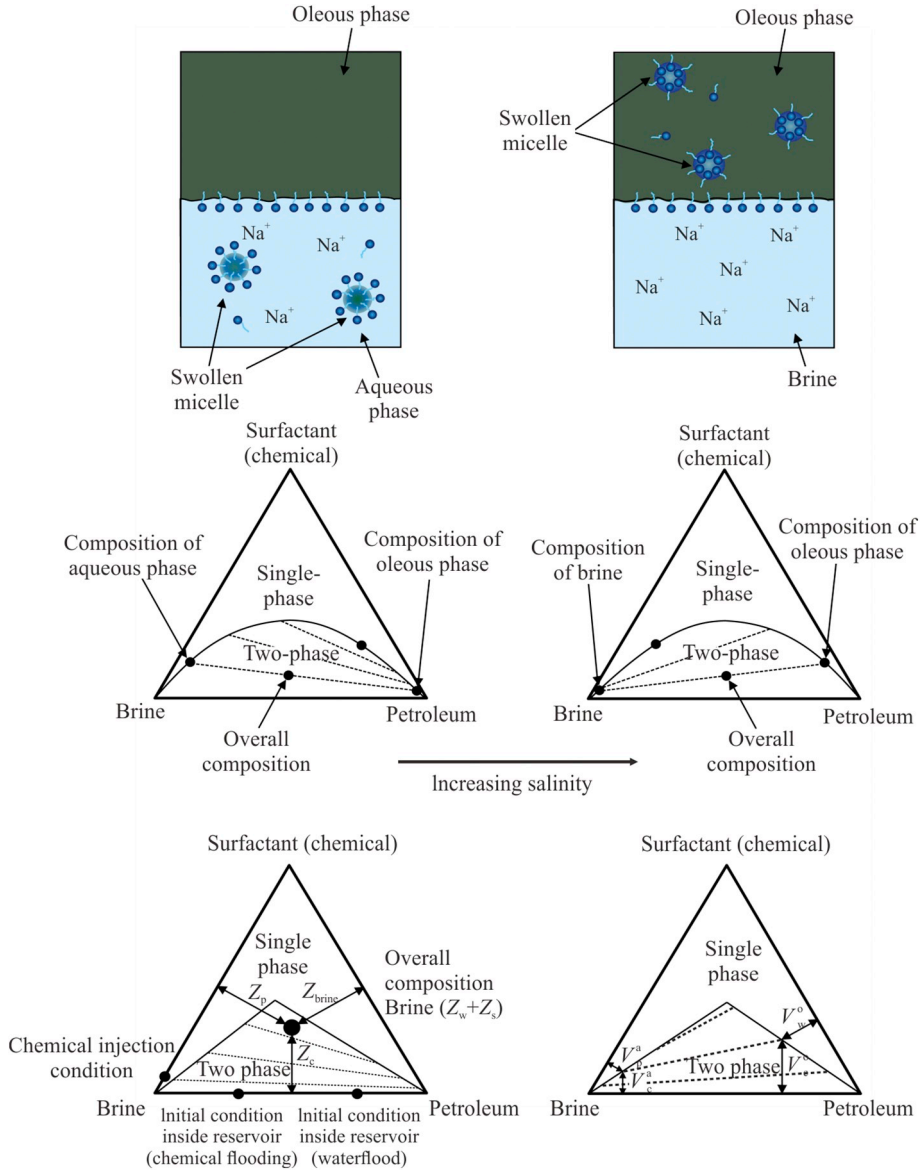

Fig. 4. Ternary phase diagrams for Type II(−) (left) and II(+) (right) systems (top) and their simplified representations (bottom) [9].

$$\frac{S^{jr}}{SjrH} = \begin{cases} 1 & \textbf{if} \quad N_{vc} < 10^{(1/T_1^j)-T_2^j} \\ T_1^j \cdot [\log(N_{vc}) + T_2^j] & \textbf{if} \quad 10^{(1/T_1^j)-T_2^j} \le N_{vc} \le 10^{-T_2^j} \\ 0 & \textbf{if} \quad N_{vc} > 10^{-T_2^j} \end{cases} \tag{13}$$

The piecewise function is defined by constant parameters which depend on the fluids and the porous medium being simulated. The relationship between the residual saturation after chemical and waterflooding processes is known as normalized residual saturation of phase *j*. The form of Eq. (13) for both phases determines what is known as capillary desaturation curves (Fig. 5). At low capillary numbers, the behavior is similar to a process of waterflooding and the normalized residual saturation is not decreased. As the IFT decreases and/or the viscosity increases, the capillary number raises to higher values than those of the secondary recovery. It is for this reason that in areas of high speeds (i.e., nearby the wells) can be achieved oil saturation values lower than those of waterflooding. As can be seen, the aqueous phase requires much higher values of N_{vc} to achieve a full desaturation [8].

2.4. Relative permeabilities

Relative permeabilities influence Darcy's equation on the phase velocities, and therefore the efficiency of oil recovery. They depend on the residual saturations which were calculated in the previous section. The model used to calculate the relative permeabilities is taken from

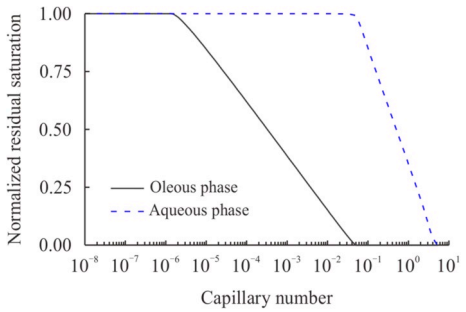

Fig. 5. Capillary desaturation curves for non-wetting (oleous) and wetting (aqueous) phases used for this simulation.

Camilleri [48,49], which is used for most chemical flooding processes. Knowing beforehand the phase saturations, the relative permeabilities are calculated according to the following formula:

$$k_r^j = k_r^{j0}\cdot\left(\frac{S^j - S^{jr}}{1 - S^{jr} - S^{j'r}}\right)^{e^j}; \quad j = o, a; \quad j \neq j' \tag{14}$$

where k_r^{j0} and e^j represent the end point and the curvature of the function $k_r^j(S^j)$. These values are calculated by the following equations:

$$k_r^{j0} = k_r^{j0H} + (1 - k_r^{j0H})\cdot\left(1 - \frac{S^{j'r}}{S^{j'rH}}\right); \quad j = o, a; \quad j \neq j' \tag{15}$$

$$e^j = e^{jH} + (1 - e^{jH})\cdot\left(1 - \frac{S^{j'r}}{S^{j'rH}}\right); \quad j = o, a; \quad j \neq j' \tag{16}$$

where k_r^{j0H} and e^{jH} are the endpoint values of curvature and relative permeability function system for water-oil without the presence of chemical agents, respectively.

2.5. Phase viscosities

The viscosity of each phase depends on its composition as a function of the volumetric concentration of each component, according to the following function [34,48,49]:

$$\mu^j = V_w^j\cdot\mu^{aH}\cdot e^{\alpha 1\cdot(V_p^j + V_c^j)} + V_p^j\cdot\mu^{oH}\cdot e^{\alpha 1\cdot(V_w^j + V_c^j)} + V_c^j\cdot\alpha_3\cdot e^{\alpha 2\cdot(V_w^j + V_o^j)}; j = o, a \tag{17}$$

where α_k are constants, and μ^{aH} and μ^{oH} are the viscosities in the water-oil system without surfactant, respectively. Nevertheless, in this work a modification is proposed to the formulation presented in simulators (e.g., UTCHEM) and the model developed by Porcelli [32], introducing the dependence on the salt in the pure water/brine viscosity and replacing the latter in Eq. (17), according to the following expression [50],

$$\mu_{brine} = \mu^a\cdot\left(1 + A_{sal}V_s^a + B_{sal}V_s^{a^2}\right) \tag{18}$$

where A_{sal} and B_{sal} are constants based on rheology experiments. For the oil phase, as did before, a Newtonian behavior is adopted. According to the literature [51], light and medium oil cuts exhibit Newtonian behavior while heavy oil might present a slight shear-thinning region.

2.6. Adsorption

The adsorption process occurs when surfactant monomers and/or micelles form onto the surface of the formation rock. In order for these monomers to aggregate and form the micelles, the surfactant concentration must exceed the critical micelle concentration (CMC). This phenomenon will cause a loss of surfactant in the porous medium, making the whole process economically unfeasible in case of high rates of adsorption [52,53]. The isotherm is rather dependent on the type of surfactant, the characteristics of the rock and the type of electrolytes present in the solution [54]. The adsorption of the surfactant by the rock used in this simulator is described by the Langmuir monolayer model [55]:

$$Ad_c = \min\left[(Z_c + Ad_c), \frac{a_{1,c}\cdot Z_c}{1 + a_{2,c}\cdot Z_c}\right] \tag{19}$$

where a_1 and a_2 are adsorption parameters and Ad_c is a dimensionless parameter representing the adsorbed volume of chemical component per unit of volume of the porous media. Since it was assumed the fluids are incompressible, adsorption is formulated on a volume basis. The term a_1 is a function of the salinity present in the reservoir, and a_2 is used to describe the adsorption process: when $a_2 = 0$ is linear adsorption, and $a_2 \neq 0$ represents a Langmuir adsorption process. The main difference in the latter lies in the fact that linear adsorption does not limit the amount of surfactant loss in the rock whilst, as a_2 increases, the maximum adsorption losses are diminished.

$$a_1 = (a_{11} + a_{12}C_{SE}) \tag{20}$$

$$C_{SE} = V_s^a\cdot\frac{1}{1 - \beta_{div}f_{div}}\cdot\frac{1}{1 + \beta_{temp}(T - T_{ref})} \tag{21}$$

The terms a_{11} and a_{12} are constant parameter obtained from laboratory experiments and C_{SE} is the effective salinity. The latter takes into account the concentration of dissolved salts in the aqueous phase, thermal effects and the fraction of total divalent cations bound to surfactant micelles [35].

2.7. Capillary pressure

The capillary pressure is defined as the difference between the non-wetting (oleous) and the wetting (aqueous) phases. This parameter is usually defined as a function of the water saturation. In this paper this relationship is described by the following power-law equation [8]:

$$p_c = C\cdot\sqrt{\frac{\varphi}{K}}\cdot\frac{\sigma}{\sigma^H}\cdot\left(\frac{1 - S^a - S^{or}}{1 - S^{ar} - S^{or}}\right)^n \tag{22}$$

where C is a constant parameter and n defines the curvature of the function. The capillary pressure parameter C relates the capillary forces in the three component system (petroleum, water and chemical) to the capillary forces in the oil-water system.

3. Results and discussions

3.1. Introduction

The proposed surfactant flooding in this paper begins in an oil field which has been exploited during secondary recovery, rendering the oil saturation close to the residual value. The reason behind this was to study in more detail how the surfactant can mobilize the remaining oil, counteracting the capillary trapping and increasing the overall performance in the reservoir. After the initial surfactant slug a water bank is used to drive the chemical agent and the oil bank towards the producing wells. The first stage of simulations in this paper comprises only the physical phenomena under study, without the influence of the salt. the second part will include the latter, presenting the results and a brief discussion of its influence in the recovery process when the adsorption is also considered.

3.1.1. Data

In order to perform the simulations, a series of properties were established aimed at emulating a EOR recovery process in an oil reservoir, showing as well the operating conditions for the wells (Tables 1–3).

3.2. Three-component system

The first part of the study of the process was carried out considering negligible the influence of the salt in the partitioning component, phase behavior and adsorption processes. The goal is to determine the influence of these phenomena on the oil recovery process. Subsequently, this fourth component was added to the system in order to determine its influence on the above-mentioned parameters. This section also includes the results of flooding processes considering several factors, namely: random permeability fields, diffusion, capillary pressure and adsorption. It is well known from previous studies that the phase behavior parameters are the most important factors affecting the recovery efficiency [9]. This study is focused then in complement this previous analysis, extending it to all the physical phenomena present in EOR processes. The latter will be used as reference case for the analysis when salt is considered and thus affects adsorption parameters in the

Table 1
Physical and numerical parameters.

Geometrical Data of the Reservoir					
Total length axis X	500 m	Total length axis Y	500 m	Field thickness	5 m
n_x elements	25	n_y elements	25 blocks		
Rock Properties					
Porosity	0.25	k_{xx}	200 mD	k_{yy}	200 mD
Initial Conditions					
S_o	0.36	S_o^r (EOR)	0.35	$S_a^{rH} = S_o^{rH}$	0.15
Simulation Data					
Total time	6000 days	Chem. inj. time	200 days	z_{clN}	0.025
Physical Data of the Phases					
μ^{aH}	1 cP	μ^{oH}	5 cP	Oil density	850 kg/m^3
Water density	1020 kg/m^3	IFT	50 mN/m		

Table 2
Wells operating parameters.

Physical Data					
Number of wells	2	Well radius	0.25 m	Skin factor	0
Operating Conditions					
Total flowrate	1650 STB/day	Bottomhole pressure	55160 kPa		

mathematical model.

3.2.1. Influence of the rock compressibility

As described in the introduction, the permeable rock formations of porous media are subject to a stress state caused by the pressure of fluid contained therein, plus the burden of the rock structure atop of it. This stress-state causes a deformation resulting in the modification of the pore volume, and therefore affects the fluid flow during oil recovery processes. Previous publications [9,31,56–58] do not consider this phenomenon, which could lead in certain cases to a significant difference in both the final values obtained, and also in the time necessary to achieve those values. In this model the rock compressibility was included to take account this phenomenon and also to study its influence on the recovery efficiency in surfactant EOR. This alters the nature of pressure equation, transforming it into a system of parabolic PDE (when the compressibility is zero, the system becomes elliptical).

In order to study the influence of the compressibility, different possible values were evaluated for rock formations, presented in Table 4 and Fig. 6, based on previous literature, without varying the phase behavior parameters, since they are independent of the mechanical properties of the porous medium.

The oil recovery values are significantly lower as the compressibility is increased (Fig. 6 - top left and Fig. 7). This is because that increasing the pore volume decreases the phase velocity in the formation, which reduces the capillary numbers of each phase, and desaturation of the oil phase decreases. However, the most affected parameter is the recovery time as well as the chemical breakthrough occurrence (Fig. 6 - top right). Both exhibit a marked dependence on compressibility values for $c_r > 7.25 \times 10^{-9}\ 1/Pa$. As the latter decreases the values approach to those from the reference case ($c_r = 0$). Pressure drop values were also influenced by the compressibility (Fig. 6 - bottom), and although they did not significantly change their values, their occurrence times did.

Table 4
Oil recovery efficiency as a function of the rock compressibility.

c_r	k_c	$L_{pc}^a = L_{wc}^o$	Oil recovered	
	–	–	m^3	%OOIP
1.45	0.5	1	42030	37.4
145	0.5	1	41809	37.2
725	0.5	1	39976	35.5
1450	0.5	1	37776	33.6

Figs. 7 and 8 show the oil saturation and rock formation porosity, respectively, for different stages of the recovery process. As can be seen in Fig. 8, compressibility values lower than $1.45 \times 10^{-9}\ 1/Pa$ generate variations in porosity considered negligible in the final simulation. Nonetheless, when $c_r = 7.25 \times 10^{-9}\ 1/Pa$ and $c_r = 1.45 \times 10^{-8}\ 1/Pa$, these values are significantly different from the reference porosity and so are the production and recovery values. The porosity and thus the total pore volume is also time dependent, as it depends on the reservoir pressure. In case of surfactant flooding this variation may be noticeable, but only in the case of high compressibilities. In different EOR processes (e.g. polymer flooding) the pressure drop due to the polymer injection could render higher variation, especially in the injection well area, which cannot be longer neglected. The shape and values on these profiles (Fig. 6 - top left and 8) do not change significantly and only differences in the final values are observed as well as the time required to achieve them, as already mentioned above.

3.2.2. Influence of the diffusion coefficient

The dispersion of the chemical species is described through the dispersion coefficient in the continuity equation as a result of the application of Fick's law to multiphase flow in porous media [34,59]. However, in this case the surfactant may be present in both phases, so the coefficient for dispersion in the oil phase is added. The results of its influence are shown in Table 5 and Fig. 9 for different values of the dispersion coefficients. The influence of this phenomenon with respect to the advective component is represented by the dimensionless Peclet number. For high values of Pe, dispersion becomes negligible and the mass transport is driven only by advective phenomena. When $Pe \approx 1$, the dispersion is of the same order as the advective terms and therefore should be taken into account in the model [9]. In this study we have assumed negligible the longitudinal and transversal components of the dispersion tensor (Eq. (3)). Moreover, previous first-order simulators added a numerical diffusion component to the solution of Eq. (2), which caused a similar effect to the physical diffusion, decreasing the recovery efficiency. This problem was solved in this simulator, which uses a second-order discretization scheme with a TVD flux-limiter function, decreasing noticeably the influence of numerical effects.

The increase in D disperses the chemical slug and the peak value of

Table 3
Auxiliary parameters used for the simulations.

IFT				Capillary Pressure				Adsorption			
G_1	−1.7	G_2	−0.02	C	0	n	1	a_1	0	a_2	0
Viscosity				**Residual Saturation**				**Relative Permeabilities**			
α_1	0	α_2	0	T_1^o	−0.25	T_1^a	−0.50	k_r^{oH}	1	k_r^{aH}	0.2
α_3	1			T_2^o	1.57	T_2^a	−0.70	e^{oH}	1.5	e^{aH}	1.5

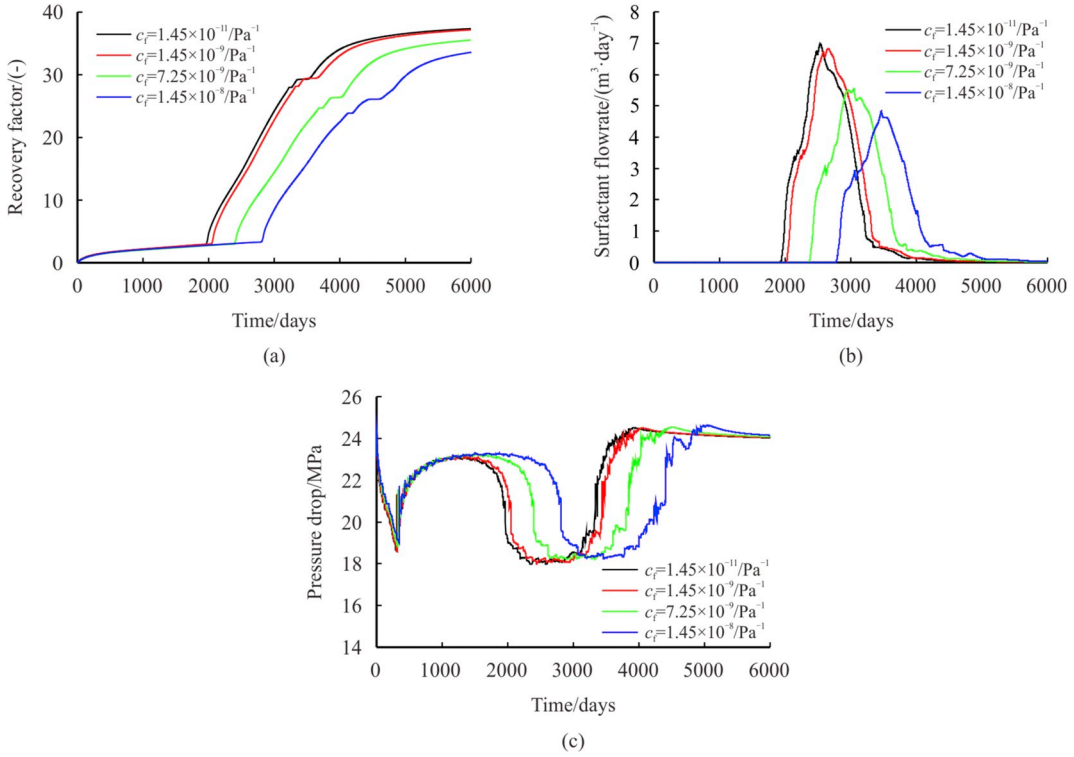

Fig. 6. Oil recovered (top left), surfactant flowrates (top right), and pressure drop (bottom) as a function of time for different rock compressibilities in a surfactant flooding.

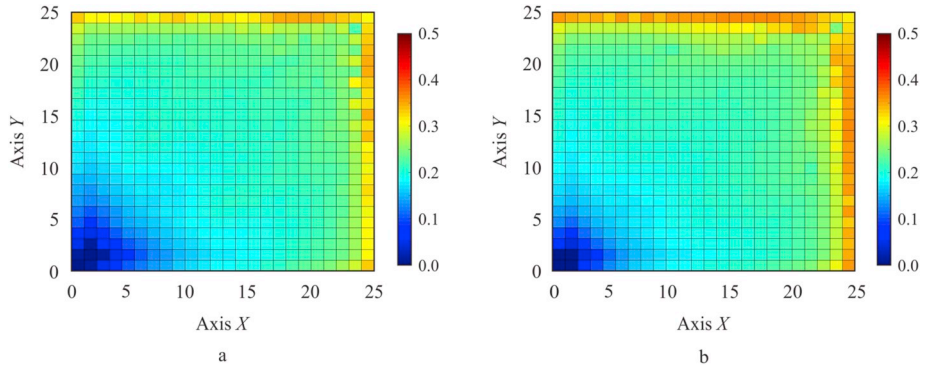

Fig. 7. Oil saturation profiles at the end of the EOR process for $c_r = 1.45 \times 10^{-11} 1/Pa$ (left) and $c_r = 1.45 \times 10^{-8}\ 1/Pa$ (right).

the chemical slug plummets. Thus, the petroleum concentration profiles are also dispersed and slightly delayed, such as reported by Porcelli [33]. The effect of dispersion of the surfactant causes a decrease in the recovery factor, rendering higher oil residual saturations after the EOR process. In the case of polymer EOR flooding, this is due to a decrease in the viscosifying properties; in a surfactant flooding, the decrease is due to the interfacial properties, which are function of the surfactant concentration. The increased dispersion also causes the chemical breakthrough occurs first, but surfactant peak flowrates decrease. This causes the flow of oil in the producing well be higher during early stages of the

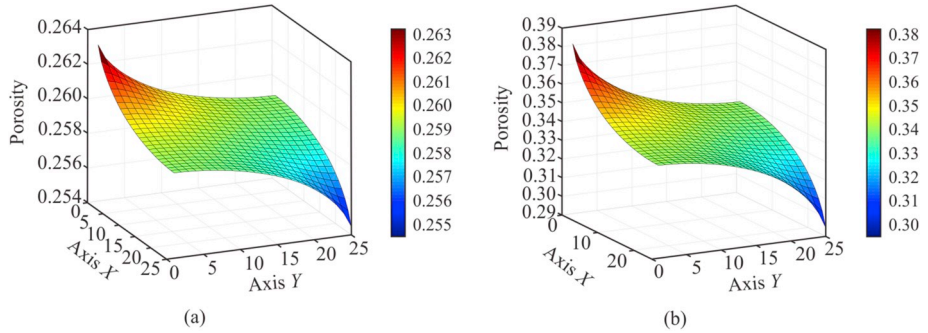

Fig. 8. Rock formation porosity profiles at the end of the EOR process for $c_r = 1.45 \times 10^{-9} 1/Pa$ (left) and $c_r = 1.45 \times 10^{-8}\ 1/Pa$ (right).

Table 5
Oil recovery efficiency as a function of the rock diffusion coefficient.

D_c	k_c	$L_{pc}^a = L_{wc}^o$	Oil recovered		D_c	k_c	$L_{pc}^a = L_{wc}^o$	Oil recovered	
	–	–	m^3	%OOIP	m^2/s	–	–	m^3	%OOIP
5	0.5	1	42434	37.7	5	2	1	71392	63.5
10	0.5	1	38827	34.5	10	2	1	66268	58.9
20	0.5	1	33791	30.0	20	2	1	60003	53.3

simulation but then, when the chemical concentration decreases, oil is trapped and the final recovery efficiency declines. This is shown in Figs. 10 and 11, where petroleum and chemical profiles are presented for different values of dispersion coefficients. This behavior also occurs for different values of phase partitioning parameters and in Type II (+) emulsion systems the reduction in the recovery efficiency is increased, which was verified in the simulator (Fig. 11). The occurrence of the chemical breakthrough is also affected differently as a function of the emulsion type (Fig. 9), with the Type II (+) water-in-oil emulsions being more affected by the dispersion tensor.

3.2.3. Influence of the capillary pressure

In this section the results of the study of the capillary pressure are presented along with its influence on oil recovery processes with chemicals. The parameters in Eq. (22) were selected according to previous literature [29,33,35,60], and the results are presented in Table 6. The maximum value for the capillary pressure is reached when the water saturation is at its residual value, whilst it becomes zero when the oil saturation is equal to its residual saturation value.

When the capillary pressure is taken into account, numerical instabilities appear in 1D models [33,34]. Porcelli [33] described this problem clearly as the stability limit is a function of the derivative dP_c/dS (in case of incompressible rock formation with constant permeability fields). In the paper, she modified the spatial grid increasing numerical diffusion in order to achieve numerical stability. The decrease of the grid in a first-order scheme caused an increase in the influence of the numerical diffusion, which also helped to achieve the stability. During this research with a 2D model, no significant stability problems were found with the grid chosen, which may be in part related to the numerical scheme used. These simulations were performed using different constants values for the two possible types of two-phase emulsions. These values are consistent with those previously reported by Porcelli regarding the sensitivity to the capillary pressure in systems Type II(−) and II(+).

The influence of the capillary pressure in oil recovery with surfactants in Type II(−) emulsions is negligible and the values obtained are virtually identical, both in chemical and oil breakthroughs occurrence as well as in the final recovery efficiency. In the case of Type II(+) systems, the influence of the capillary pressure becomes more noticeable, although its effect is much lower compared to those from the phenomena studied earlier in this paper (Table 6). Oil and chemical breakthroughs occur before those taken as reference. As in the case of the 1D model, the capillary pressure remains constant both before and after the chemical slug: in the first case is the value of the capillary pressure for the system with the oil saturation after waterflooding; in the second, since the oil saturation is at its residual value, the capillary pressure is zero. It is only in the chemical bank that capillary pressure values vary (Fig. 12).

As conclusion, in a chemical surfactant flooding process in reservoir-scale models, with high pressures, capillary pressure can be neglected without making significant mistakes in the numerical simulation. However, in laboratory-scale models, with very low injection pressures, capillary pressure effects should be considered when the phase behavior represents a Type II(+) emulsion. For systems Type II (−) it can be also neglected without making major mistakes in the results and times obtained regarding the oil recovered.

3.2.4. Influence of adsorption

The last part of this section dealing with a three-component simulator aims at presenting the influence of adsorption in a surfactant EOR process. The adsorption can significantly affect the process of a chemical EOR flooding, both from a technical and economical perspectives. In order to study the effects from the point of view of the recovery factor, several simulations were performed varying the parameters in Eq. (19) (Table 7 and Fig. 13). A reference case without adsorption was taken as a benchmark for the study. The parameter a_1 determines the level of adsorption of the chemical in the rock, determined by the physical and chemical properties of both. The parameter a_2 determines the type of adsorption process: linear or Langmuir.

The adsorption causes a detriment in the recovery efficiency, and has a much greater influence than the other physical phenomena presented here. This is evidenced in a greater extent during a linear adsorption process (Fig. 13). These results and trends coincide with those presented previously [9], as well as those results reported by Porcelli and Bidner [31,33,34,56]. The adsorption process decreases the recovery efficiency and delays the occurrence of chemical and oil breakthroughs (Fig. 14). It is noteworthy the difference in the last one is not due to a modification of the surfactant slug velocity but for the amount of surfactant reaching the producing well, since it is evident from Fig. 14 that the peak in the concentration at the well remains practically unaltered.

The maximum values of chemical concentration and their point of occurrence for a given time change according to the values of the constants a_1 and a_2. The maximum value is inversely-proportional to a_1 and directly-to a_2. The chemical bank is delayed by the phenomenon of adsorption, retarding its breakthrough in the producing well. This phenomenon is more pronounced for Type II(+) emulsions, where the influence of adsorption became more noticeable (Fig. 15). This was already noted by Porcelli [33] in a 1D model. The cause of such increase in the sensitivity is that in such systems the major concentration of chemical is present in the oil phase, which moves in the porous medium at a lower velocity than the aqueous phase, thus increasing the

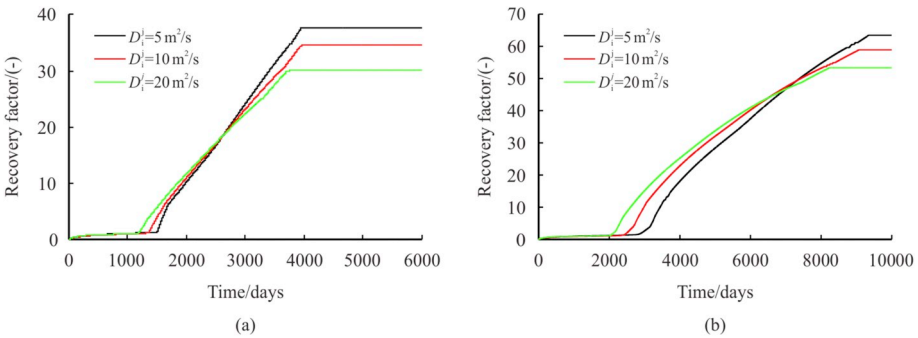

Fig. 9. Oil recovered in Type II(−) (left) and Type II(+) (right) as a function of time for different diffusion coefficients in a surfactant flooding.

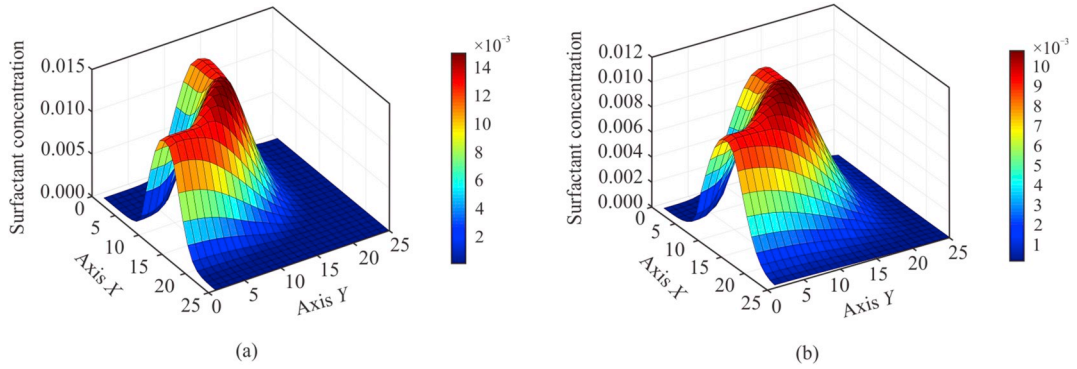

Fig. 10. Surfactant concentration (after 1000 days) considering a diffusion coefficient of $D = 5\,m^2/s$ (left) and $D = 10\ m^2/s$ (right) with a Type II(−) emulsion.

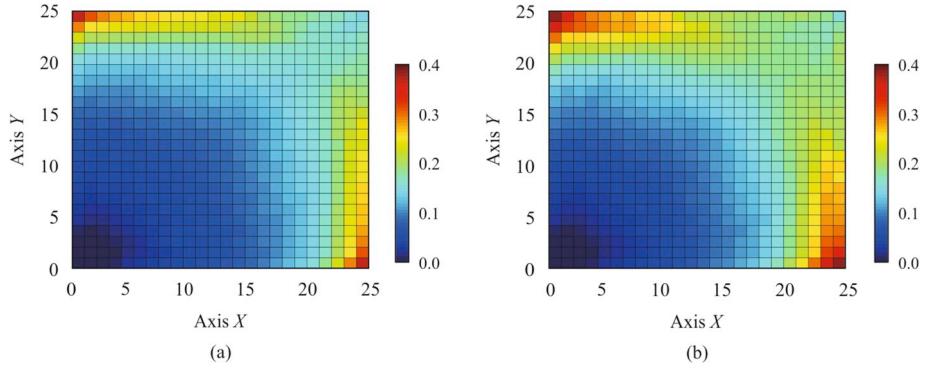

Fig. 11. Oil saturation profiles at the end of the EOR process considering a diffusion coefficient of $D = 5\,m^2/s$ (left) and $D = 10\ m^2/s$ (right) with a Type II(+) emulsion.

Table 6
Oil recovery efficiency as a function of capillary pressure.

k_c	$L^a_{pc} = L^o_{wc}$	C	Oil recovered	
–	–	$kPa{\cdot}m$	m^3	%OOIP
0.5	1	0	42160	37.5
0.5	1	30000	41505	36.9
2	1	0	75931	67.5
2	1	15000	74792	66.5
2	1	30000	74623	66.3

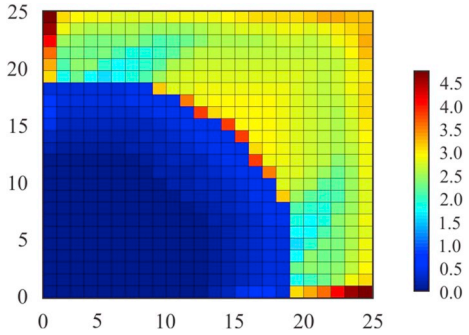

Fig. 12. Capillary pressure profile (in kPa) after 3000 days for a Type II(+) emulsion, with $C = 30000 kPa{\cdot}m$.

rate of adsorption. This influence is directly proportional to the partition coefficient (Figs. 15 and 16). Therefore, for such systems, this phenomenon should be carefully studied and analyzed as it could lead to the total failure of the recovery processes with surfactants. This will depend on the characteristics of the rock formation and the surfactant type (e.g. anionic, zwitterionic) but it is recommended that the

Table 7
Oil recovery efficiency as a function of the adsorption coefficients for different types of emulsion and adsorption processes.

k_c	a_1	a_2	Oil recovered		k_c	a_1	a_2	Oil recovered	
–	–	–	m^3	%OOIP	–	–	–	m^3	%OOIP
0.5	0	0	42160	37.5	2	0	0	75931	67.5
0.5	0.15	3	37589	36.9	2	0.15	3	65755	58.5
0.5	0.25	3	28846	67.5	2	0.25	3	49148	43.7
0.5	0.6	3	12540	66.3	2	0.6	3	15208	13.5

adsorption should not be neglected in surfactant EOR processes. Moreover, the design of novel agents should consider the adsorption rates as one of the key parameters during the synthesis and subsequent testing.

3.3. Four-component system

The second part of this study comprises the study and discussion of an EOR process considering a fourth component, namely the salt. On this simulator there is no difference between mono- or divalent salt ions in the simulator, although it is reported in the literature that divalent cations have a more significant influence in the surfactant adsorption rates. This difference cannot be neglected if the brine used during the EOR process or the content of salts in the reservoir presents a significant percentage of divalent cations. The scope of the study in this paper is to analyze the influence of salt content on the adsorption of chemical species onto the rock formation. The simulations performed in this section considered a porous media with several initial salt contents, both below and above the critical salt concentration. This describes the possible two-phase systems in porous media, Type II(+) and II(−), together with different contents of salt in the injection water (brine), in

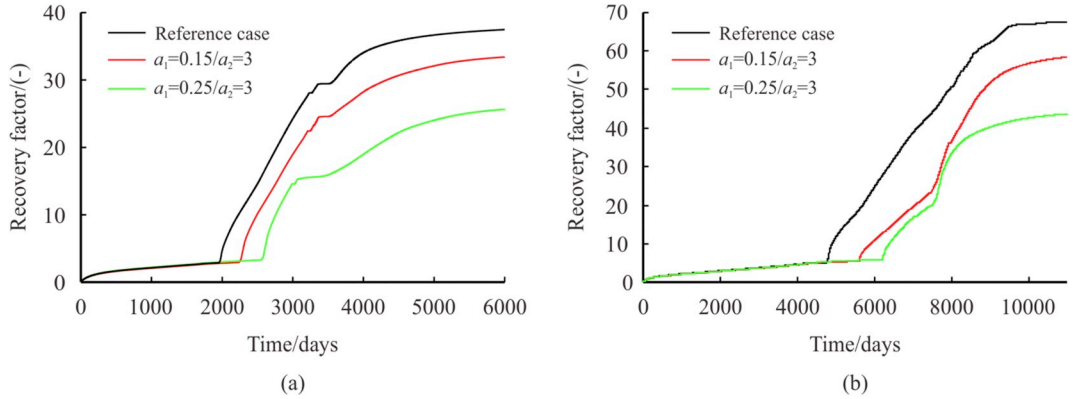

Fig. 13. Oil recovered in Type II(−) (left) and Type II(+) (right) as a function of time for different adsorption rates and processes, compared to the respective reference cases.

order to study the influence of salinity with the injection process [61]. In the adsorption this was taken into account considering the salt content in the constant a_1 (Eqs. (20) and (21)), analyzing different values of the parameter a_{12}. These results were then compared to those obtained in a reference case (without adsorption).

3.3.1. *Influence of the salt component on the adsorption*

The final series of simulations in this paper are aimed at studying the influence of adsorption when the salt is considered in the system. This affects Eq. (20), specifically the parameter a_{12}. Since an isothermal system is assumed and moreover the presence of divalent cations is negligible, the effective salinity is equal to the salt concentration in the aqueous phase (Eq. (21)). This influence was studied considering different values for the variable a_{12}, under similar operational and salinity conditions (Table 8 and Fig. 17). For all the cases, it was assumed the same initial salt content in the reservoir, but the brine injected was modified, modifying therefore the partition coefficient and the emulsion type.

As in the three-component system, the phenomenon of adsorption causes a detriment in the recovery efficiency, which has both operational and economic consequences. As expected, the recovery factor is inversely proportional to the values of a_{12} (Fig. 17). The objective is to determine the degree of influence of this phenomenon and this variable in the whole adsorption process. When the salt content originates Type II(+) emulsions in the reservoir, the adsorption influences more significantly than when the salt is below the critical value, creating Type II (−) emulsions. The cause of this major influence was already explained in the previous section (see point 3.2.4) and is due to the degree of chemical partition and the Darcy phase velocities in the rock formation. As concluded previously, the adsorption must be studied carefully before starting a process of chemical EOR, as incorrect estimation of these values may result in the total failure of the process. This effect should be considered in further detail when using surfactant which create water-in-oil emulsions, since the chemical partition and the phase velocities increase the adsorption losses, which ultimately affects to a greater extent the recovery factor.

4. Conclusions

This paper aimed at extending the study of a novel surfactant flooding simulator, considering the influence of the different physical phenomena present in underground media. With this respect, a previously published two-dimensional simulator for four pseudo-components, two phase flow, was applied to a series of EOR processes. The physical model was described and later discretized using a system of non-linear differential equations, solved by the finite differences method, with an algorithm which was implemented in MathWorks MATLAB®. The second-order numerical scheme coupled with the TVD flux limiter functions allowed reducing the numerical errors and the appearance of artificial diffusion and dispersion phenomena in the chemical front tracking.

The simplification of the ternary diagram showed to be a valid approach to model a surfactant process in a simple, but accurate way. The phenomena studied in this paper affected negatively the recovery process, when compared to ideal, benchmark cases. From all these effects the most relevant in terms of a decrease in the oil recovery factor was the adsorption of the surfactant onto the rock formation. This was more noticeable in Type II(+) emulsions (water-in-oil), due to the

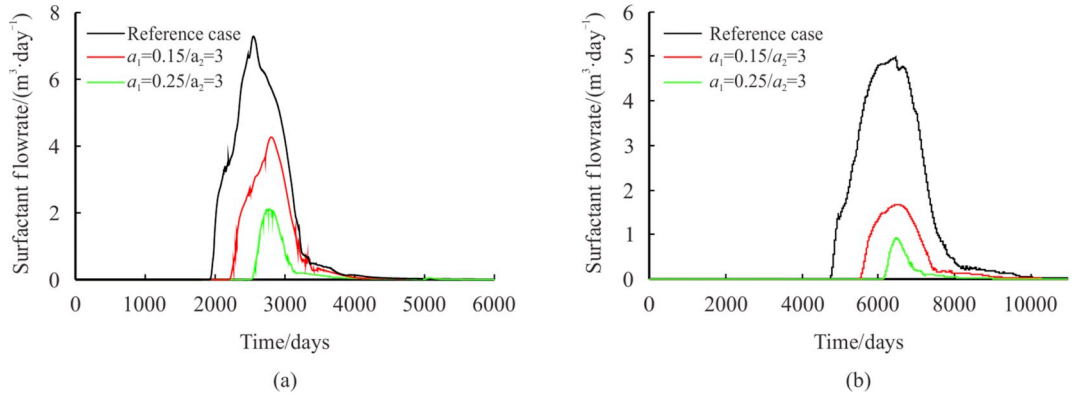

Fig. 14. Surfactant produced flowrates as a function of time for a Type II(−) (left) and Type II(+) (right) emulsions under different adsorption rates, compared to the respective reference case.

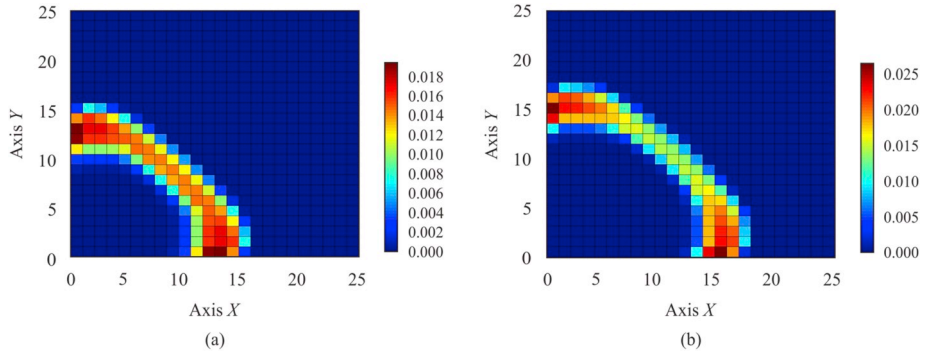

Fig. 15. Surfactant concentration in a Type II(−) emulsion after 1000 days with $a_1 = 0.25$ (left), and a Type II(+) emulsion after 3000 days with $a_1 = 0.25$ (right).

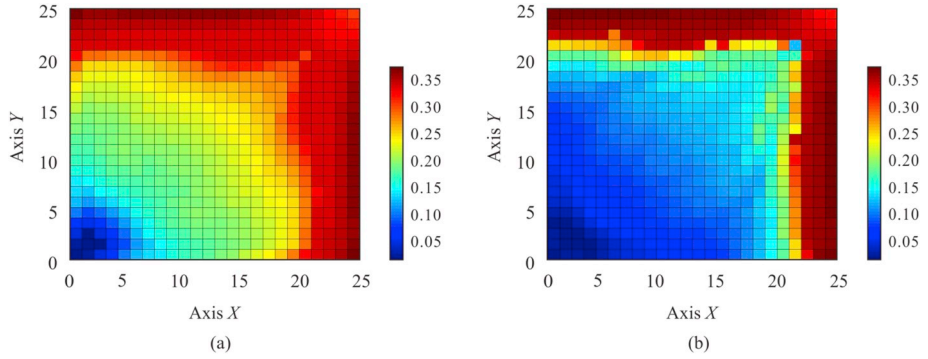

Fig. 16. Oil concentration at the end of the EOR process in a Type II(−) emulsion with $a_1 = 0.25$ (left), and a Type II(+) emulsion with $a_1 = 0.25$ (right).

Table 8
Oil recovery efficiency as a function of the parameter a_{12}, considering the adsorption process in the reservoir.

Initial salt content	Critical salt content	Salt injected	a_{11}	a_{22}	Oil recovered	
%	%	%	–	–	m^3	%OOIP
1.5	2	0.5	0.05	0	38419	34.2
1.5	2	0.5	0.05	2.5	36660	32.6
1.5	2	0.5	0.05	5	35573	31.6
1.5	2	1	0.05	0	48641	43.2
1.5	2	1	0.05	2.5	41706	37.1
1.5	2	1	0.05	5	32123	28.6

effect of the loss of chemical into the porous medium. The capillary pressure, on the other hand, did not play a significant role in the recovery process, hence it can be neglected when EOR processes are being simulated. The addition of the salt as a fourth component influenced more notoriously the recovery process in Type II(+) emulsions, whilst in Type II(−) the reduction in the recovery performance was significantly lower.

All in all, even though the numerical validation has been done, future work is considered necessary before a full field-scale application of this model is carried out. It is deemed that lab-scale experiments should be done in 2D or 3D models with surfactants to demonstrate the applicability and potential of this novel EOR simulator. Core flooding is also recommended, though it is advisable the employment of physical models in which the area and volumetric sweeping efficiencies can be also analyzed. Thus, this will allow setting the EOR agent parameters in an accurate way before a field-scale application is pursued in order to design novel EOR products. Surfactant EOR simulations showed the potential of EOR methods to sweep the residual oil by means of reducing the IFT. The model employed with the ternary diagram may provide a simple way to design chemical surfactant with specific properties before experimental or field tests are performed.

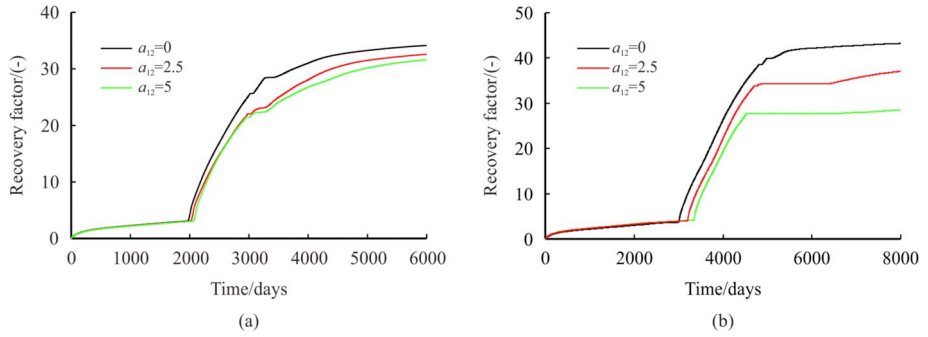

Fig. 17. Oil recovered as a function of time for different sets of initial and injected salt concentrations along with the adsorption process: 1.5/0.5% (left) and 1.5/1.0% (right).

Acknowledgments

P.D. gratefully acknowledges the support of the Erasmus Mundus EURICA scholarship program (Program Number 2013-2587/001-001-EMA2) and the Roberto Rocca Education Program.

Appendix A. Supplementary data

Supplementary data to this article can be found online at https://doi.org/10.1016/j.petlm.2019.07.001.

References

[1] N.A. Owen, O.R. Inderwildi, D.A. King, The status of conventional world oil reserves-Hype or cause for concern? Energy Policy 38 (8) (2010) 4743–4749, https://doi.org/10.1016/j.enpol.2010.02.026.
[2] BPplc, Statistical Review of World Energy June 2014, Annual Report 63, (2014) BP p.l.c. http://www.bp.com/en/global/corporate/about-bp/energy-economics/statistical-review-of-world-energy.html.
[3] L.P. Dake, Fundamentals of Reservoir Engineering, Elsevier, Amsterdam, the Netherlands, 0-444-41830-X, 1978.
[4] M.S. Bidner, Propiedades de la Roca y los Fluidos en Reservorios de Petroleo, EUDEBA, Buenos Aires, Argentina, 950-23-1150-7, 2001.
[5] A. Satter, G.M. Iqbal, J.L. Buchwalter, Practical Enhanced Reservoir Engineering, PennWell Books, Tulsa, USA, 978-1-59370-056-0, 2008.
[6] R.L. Schmidt, P.B. Venuto, L.W. Lake, A Niche for enhanced oil recovery in the 1990's, Review (1) (1992) 55–61.
[7] G.J. Hirasaki, C.A. Miller, M. Puerto, Recent advances in surfactant EOR, SPE J. 16 (4) (2011) 889–907, https://doi.org/10.2118/115386-PA.
[8] L.W. Lake, Enhanced Oil Recovery, Prentice-Hall Inc., Englewood Cliffs, USA, 0-13-281601-6, 1989.
[9] P. Druetta, J. Yue, P. Tesi, C.D. Persis, F. Picchioni, Numerical modeling of a compositional flow for chemical EOR and its stability analysis, Appl. Math. Model. 47 (2017) 141–159, https://doi.org/10.1016/j.apm.2017.03.017.
[10] P. Druetta, P. Tesi, C.D. Persis, F. Picchioni, Methods in oil recovery processes and reservoir simulation, Adv. Chem. Eng. Sci. 6 (04) (2016) 39, https://doi.org/10.4236/aces.2016.64039.
[11] P. Druetta, F. Picchioni, Numerical modeling and validation of a novel 2D compositional flooding simulator using a second-order TVD scheme, Energies 11 (09) (2018) 2280, https://doi.org/10.3390/en11092280.
[12] H.E. Garrett, Surface Active Chemicals, first ed. edn., Pergamon Press, New York, USA, 0-08-016422-6, 1972.
[13] H.H. Farrell, M.D. Gregory, M.T. Borah, Progress Report: Big Muddy Field Low-Tension Flood Demonstration Project with Emphasis on Injectivity and Mobility, MS, 1984, https://doi.org/10.2118/12682.
[14] T.R. Reppert, J.R. Bragg, J.R. Wilkinson, T.M. Snow, N.K. M Jr., W.W. Gale, Second Ripley Surfactant Flood Pilot Test, (1990), https://doi.org/10.2118/20219-MS.
[15] J.M. Maerker, W.W. Gale, Surfactant flood process design for Loudon, SPE Reserv. Eng. 7 (1) (1992) 36–44, https://doi.org/10.2118/20218-PA.
[16] D.W. Green, G.P. Willhite, Enhanced Oil Recovery, Society of Petroleum Engineers, Richardson, USA, 978-1-55563-077-5, 1998.
[17] S. Iglauer, Y. Wu, P. Shuler, Y. Tang, I. Goddard, A. William, New surfactant classes for enhanced oil recovery and their tertiary oil recovery potential, J. Pet. Sci. Eng. 71 (1–2) (2010) 23–29, https://doi.org/10.1016/j.petrol.2009.12.009.
[18] J.J. Sheng, Status of surfactant EOR technology, Petroleum 1 (2) (2015) 97–105, https://doi.org/10.1016/j.petlm.2015.07.003.
[19] R.G. Larson, H.T. Davis, L.E. Scriven, Elementary mechanisms of oil-recovery by chemical methods, J. Pet. Technol. 34 (2) (1982) 243–258, https://doi.org/10.2118/8840-PA.
[20] R.M. Pashley, M.E. Karaman, Surfactants and Self-Assembly, Applied Colloid and Surface Chemistry, John Wiley & Sons, Ltd, 978-0-47001-470-7, 2005, pp. 61–77, https://doi.org/10.1002/0470014709.ch4.
[21] C. Negin, S. Ali, Q. Xie, Most common surfactants employed in chemical enhanced oil recovery, Petroleum 3 (2) (2017) 197–211, https://doi.org/10.1016/j.petlm.2016.11.007.
[22] T.W. Teklu, W. Alameri, H. Kazemi, R.M. Graves, A.M. AlSumaiti, Low salinity water-Surfactant-CO2 EOR, Petroleum 3 (3) (2017) 309–320, https://doi.org/10.1016/j.petlm.2017.03.003.
[23] B. Adibhatla, K.K. Mohanty, Parametric analysis of surfactant-aided imbibition in fractured carbonates, J. Colloid Interface Sci. 317 (2) (2008) 513–522, https://doi.org/10.1016/j.jcis.2007.09.088.
[24] S. Akin, A.R. Kovscek, Computed tomography in petroleum engineering research, Geol. Soc. London, Spec. Publ. 215 (1) (2003) 23–38, https://doi.org/10.1144/GSL.SP.2003.215.01.03.
[25] S. Keshtkar, M. Sabeti, A.H. Mohammadi, Numerical approach for enhanced oil recovery with surfactant flooding, Petroleum 2 (1) (2016) 98–107, https://doi.org/10.1016/j.petlm.2015.11.002.
[26] M. Lotfollahi, A. Varavei, M. Delshad, R. Farajzadeh, G.A. Pope, Development of a hybrid black-oil/surfactant enhanced oil recovery reservoir simulator, J. Pet. Sci. Eng. 133 (2015) 130–146, https://doi.org/10.1016/j.petrol.2015.05.008.
[27] S.K. Nandwani, M. Chakraborty, S. Gupta, Chemical flooding with ionic liquid and nonionic surfactant mixture in artificially prepared carbonate cores: a diffusion controlled CFD simulation, J. Pet. Sci. Eng. 173 (2019) 835–843, https://doi.org/10.1016/j.petrol.2018.10.083.
[28] J.S. Nolen, Numerical Simulation of Compositional Phenomena in Petroleum Reservoirs, MS, 1973, https://doi.org/10.2118/4274.
[29] G.A. Pope, R.C. Nelson, A chemical flooding compositional simulator, Soc. Pet. Eng. J. 18 (1978) 339–354, https://doi.org/10.2118/6725-PA.
[30] R.C. Nelson, G.A. Pope, Phase relationships in chemical flooding, Soc. Pet. Eng. J. 18 (1978) 325–338, https://doi.org/10.2118/6773-PA.
[31] M. Bidner, P. Porcelli, Influence of phase behavior on chemical flood transport phenomena, Transp. Porous Media 24 (3) (1996) 247–273, https://doi.org/10.1007/BF00154093.
[32] P. Porcelli, M. Bidner, Simulation and transport phenomena of a ternary 2-phase flow, Transp. Porous Media 14 (2) (1994) 101–122, https://doi.org/10.1007/BF00615196.
[33] M. Bidner, P. Porcelli, Influence of capillary pressure, adsorption and dispersion on chemical flood transport phenomena, Transp. Porous Media 24 (3) (1996) 275–296, https://doi.org/10.1007/BF00154094.
[34] M.S. Bidner, G.B. Savioli, On the numerical modeling for surfactant flooding of oil reservoirs, Mecanica Computacional XXI (2002) 566–585.
[35] M. Delshad, G. Pope, K. Sepehrnoori, UTCHEM Version 9.0 Technical Documentation, Center for Petroleum and Geosystems Engineering, The University of Texas at Austin, Austin, Texas 78751.
[36] J. Liu, M. Delshad, G.A. Pope, K. Sepehrnoori, Application of higher-order flux-limited methods in compositional simulation, Transp. Porous Media 16 (1) (1994) 1–29, https://doi.org/10.1007/BF01059774.
[37] G.J. Hirasaki, Application of the theory of multicomponent, multiphase displacement to 3-component, 2-phase surfactant flooding, Soc. Pet. Eng. J. 21 (2) (1981) 191–204, https://doi.org/10.2118/8373-PA.
[38] R.G. Larson, The influence of phase behavior on surfactant flooding, Soc. Pet. Eng. J. 19 (6) (1979) 411–422, https://doi.org/10.2118/6774-PA.
[39] J. Bear, Dynamics of Fluids in Porous Media vol. 1, American Elsevier Publishing Company, 978-0-44400-114-6, 1972.
[40] Z. Chen, G. Huan, Y. Ma, Computational Methods for Multiphase Flows in Porous Media, Society for Industrial and Applied Mathematics, ISBN isbn978-0-89871-606-1, 10.1137/1.9780898718942.
[41] D. Kuzmin, A Guide to Numerical Methods for Transport Equations, University Erlangen-Nuremberg, Germany, 2010.
[42] R. Barrett, M. Berry, T. Chan, J. Demmel, J. Donato, J. Dongarra, V. Eijkhout, R. Pozo, C. Romine, der Vorst van, Templates for the Solution of Linear Systems: Building Blocks for Iterative Methods, Society for Industrial and Applied Mathematics, 978-0-89871-328-2, 1994, https://doi.org/10.1137/1.9781611971538.
[43] K. Kamalyar, R. Kharrat, M. Nikbakht, Numerical aspects of the convection-dispersion equation, Pet. Sci. Technol. 32 (14) (2014) 1729–1762, https://doi.org/10.1080/10916466.2010.490802.
[44] D. Attwood, A.T. Florence, Surfactant Systems - Their Chemistry, Pharmacy and Biology, Chapman and Hall, London, UK, 978-9-40095-775-6, 1983.
[45] A.P. Gomora-Figueroa, R.G. Camacho-Velazquez, J. Guadarrama-Cetina, T.I. Guerrero-Sarabia, Oil emulsions in naturally fractured porous media, Petroleum (2018), https://doi.org/10.1016/j.petlm.2018.12.004 (In Press).
[46] A.A. Umar, I.B. Saaid, A.A. Sulaimon, R.B. Pilus, A review of petroleum emulsions and recent progress on water-in-crude oil emulsions stabilized by natural surfactants and solids, J. Pet. Sci. Eng. 165 (2018) 673–690, https://doi.org/10.1016/j.petrol.2018.03.014.
[47] J. Sheng, Modern Chemical Enhanced Oil Recovery, Elsevier, Amsterdam, the Netherlands, 978-0-08096-163-7, 2011.
[48] D. Camilleri, S. Engelson, L.W. Lake, E.C. Lin, T. Ohnos, G. Pope, K. Sepehrnoori, Description of an improved compositional Micellar/polymer simulator, SPE Reserv. Eng. 2 (1987) 427–432, https://doi.org/10.2118/13967-PA.
[49] D. Camilleri, A. Fil, G.A. Pope, B.A. Rouse, K. Sepehrnoori, Comparison of an improved compositional Micellar/polymer simulator with laboratory corefloods, SPE Reserv. Eng. 2 (1987) 441–451, https://doi.org/10.2118/12083-PA.
[50] H. El-Dessouky, H.M. Ettouney, Fundamentals of Salt Water Desalination, Elsevier Science, Amsterdam, the Netherlands, 978-0-08053-212-7, 2002.
[51] M.T. Ghannam, S.W. Hasan, B. Abu-Jdayil, N. Esmail, Rheological properties of heavy & light crude oil mixtures for improving flowability, J. Pet. Sci. Eng. 81 (2012) 122–128, https://doi.org/10.1016/j.petrol.2011.12.024.
[52] N. Yekeen, M.A. Manan, A.K. Idris, A.M. Samin, Influence of surfactant and electrolyte concentrations on surfactant Adsorption and foaming characteristics, J. Pet. Sci. Eng. 149 (2017) 612–622, https://doi.org/10.1016/j.petrol.2016.11.018.
[53] Y. Wu, W. Chen, C. Dai, Y. Huang, H. Li, M. Zhao, L. He, B. Jiao, Reducing surfactant adsorption on rock by silica nanoparticles for enhanced oil recovery, J. Pet. Sci. Eng. 153 (2017) 283–287, https://doi.org/10.1016/j.petrol.2017.04.015.
[54] F.D.S. Curbelo, V.C. Santanna, E.L.B. Neto, T.V. Dutra, T.N.C. Dantas, A.A.D. Neto, A.I.C. Garnica, Adsorption of nonionic surfactants in sandstones, Colloid. Surf. Physicochem. Eng. Asp. 293 (1–3) (2007) 1–4, https://doi.org/10.1016/j.colsurfa.2006.06.038.
[55] C. Thomas, P. Fleming, W. Winter, A ternary, 2-phase, mathematical-model of oil-recovery with surfactant systems, Soc. Pet. Eng. J. 24 (6) (1984) 606–616, https://doi.org/10.2118/12934-PA.
[56] A. Aulia, N.A. El-Khatib, Mathematical description of the implementation of the adaptive Newton-Raphson method in compositional porous media flow, Int. J. Basic Appl. Sci. 10 (6) (2010) 108–115.
[57] D. Bhuyan, L.W. Lake, G.A. Pope, Mathematical modeling of high-pH chemical flooding, SPE Reserv. Eng. 5 (1990) 213–220, https://doi.org/10.2118/17398-PA.
[58] Z. Chen, Y. Ma, G. Chen, A sequential numerical chemical compositional simulator,

Transp. Porous Media 68 (3) (2007) 389–411, https://doi.org/10.1007/s11242-006-9050-y.
[59] L. Lake, G. Pope, G. Carey, K. Sepehrnoori, Isothermal, multiphase, multicomponent fluid-flow in permeable media .1. Description and mathematical formulation, In Situ 8 (1) (1984) 1–40.
[60] M. Delshad, N.F. Najafabadi, G. Anderson, G.A. Pope, K. Sepehrnoori, Modeling wettability alteration by surfactants in naturally fractured reservoirs, SPE Reserv. Eval. Eng. 12 (2009) 361–370, https://doi.org/10.2118/100081-PA.
[61] T.W. Teklu, W. Chen, C. Dai, X. Li, Z. Zhou, N. Alharthy, L. Wang, H. Abass, Low-salinity water and surfactants for hydraulic fracturing and EOR of shales, J. Pet. Sci. Eng. 162 (2018) 367–377, https://doi.org/10.1016/j.petrol.2017.12.057.